GIS Odyssey Journal

2024 • Volume 4 • Number 1

https://doi.org/10.57599/gisoj.2024.4.1.79

Dawid Kwaśniak[1], Sławomir Cellmer[2]

THE STABILITY OF INTER-SYSTEM BIAS OVER TIME FOR POSITIONING USING GPS AND GALILEO

Abstract: The introduction of new overlapping signals from GPS and Galileo, such as L1 and E1 and L5 and E5a, presents new opportunities for enhanced precision and reliability in positioning. However, it also introduces new challenges that need to be addressed. One of the primary challenges in processing GPS and Galileo observations is the requirement for Inter-System Bias (ISB) handling. An important aspect has become the examination of the stability of the ISB parameter over time. Both short-term and long-term stability must be investigated. For this purpose, experiments were conducted on 20 permanent IGS stations in 10 pairs. Using the Modified Ambiguity Function Approach (MAFA) method, the stability of the ISB parameter over time was investigated, both for short-term (daily) and long-term periods. When selecting pairs, care was taken to ensure that the distances between the receivers in the pair were shorter than 10 kilometers. This allowed us to reduce the influence of the atmosphere on the obtained results. Observation data were obtained from the permanent GNSS stations mentioned above for 2020 and 2021. Calculations were conducted for the GPS and Galileo systems corresponding observations. The obtained results showed that for both the short-term period, which is a day, and for the more extended period of time (few months), the ISB exhibits significant stability. This means that once determined, the ISB can be used for several months for a given pair of receivers.

Keywords: GNSS, GPS, Galileo, Inter-System Bias, MAFA

Received: 26 April 2024; accepted: 23 July 2024

[1] University of Warmia and Mazury in Olsztyn, Faculty of Geoengineering, Department of Geodesy, Olsztyn, Poland, ORCID ID: https://orcid.org/0000-0001-6144-237X, email:dawid.kwasniak@uwm.edu.pl
[2] University of Warmia and Mazury in Olsztyn, Faculty of Geoengineering, Department of Geodesy, Olsztyn, Poland, ORCID ID: https://orcid.org/0000-0002-2614-8017, email: slawomir.cellmer@uwm.edu.pl

Introduction

The appearance of new satellite systems such as Galileo and BeiDou has created new possibilities in satellite positioning. Not only has the number of available satellites increased, but thanks to shared frequencies with GPS, the reliability and accuracy of positioning have also increased. GPS, Galileo and BDS (BeiDou System) share common frequencies: 1575.42 (L1, E1 and B1, respectively) MHz and 1176.45 MHz (L5, E5a, B2a) (Kwaśniak & Cellmer, 2021). However, along with the benefits come challenges. A specific parameter is not eliminated while creating double-differenced (DD) observations using two different satellite systems. This parameter is Inter-System Bias (ISB). ISB can also be present in code observations when using two or more satellite systems. This occurs due to the correlation process within the GNSS receiver. The code ISB can be estimated as an additional parameter. It is often estimated as part of the Single Point Positioning (SPP) model. Taking ISB parameter into account is necessary because it can reach up to several hundred nanoseconds, depending on the receivers used (Paziewski & Wielgosz, 2017). In classical methods, based on ambiguity resolution, there is a need to combine the ISB with the ambiguity of the phase measurement. Otherwise, a defect in the design matrix appears (Odijk & Teunissen, 2013). However, another method also estimates the phase ISB, but without linking the ISB with ambiguity. That method is the MAFA (Modified Ambiguity Function Approach) method (Cellmer et al., 2018). The key is to determine the value of ISB and incorporate it into the position-determination process. Especially since ISB occurs in code and phase observations and in relative (e.g. RTK) and absolute positioning (e.g. SPP, PPP). The issue of determining ISB using phase (Xu et al., 2015; Li et al., 2023; Liu, 2022) and code observations (Odijk & Teunissen, 2013; Håkansson et al., 2017; Zang et al., 2017) has been the subject of research for many years. It is also important to determine the stability of ISB over time, which is also the subject of research (Paziewski et al., 2015; Zang et al., 2019; Li et al., 2021). The authors of this article also undertook the challenge of determining the stability of ISB over time, both in the short and long term. The MAFA method has been known since 2010. However, it has never been used for an ISB estimation before. For this purpose, it was necessary to expand the mathematical model of this method. The benefits arising from using this method will be presented in the article. The calibrated ISB can also be introduced to a model as a known parameter. In this case, there is no need to estimate the ISB value.

Methods

Inter-System Bias in GNSS positioning

We can distinguish two methods for GNSS data processing using two or more systems: loose and tight combining (Paziewski & Wielgosz, 2015). In the loose combining, we choose a separate reference satellite for each system. This method is beneficial for systems that transmit signals at different frequencies. However, it can also be used when two GNSS systems transmit signals at the same frequency. In the case of tight combining, we chose only one reference satellite for all used GNSS systems. In the

case of this method, the systems should share common frequencies (Zhu & Li, 2021). Common processing of data brings benefits but also new challenges. When using only one reference satellite, we obtain one more double-differenced (DD) observation than in the loosely combined case. This can enhance the model. However, we have to consider the differences in the time and reference systems, and a new factor appears: Inter-System Bias. The ISB is caused by the correlation process in the GNSS receiver and affects both code and phase observations (Kwaśniak & Cellmer, 2021). It has a significant impact on positioning results, so it has to be considered. The observation equation for the GPS system can be written as follows (Leick et al., 2015):

$$\Phi_A^{G1} = \frac{1}{\lambda}\rho_A^{G1} + (dt_A - dt^{G1}) + \frac{1}{\lambda}T_A^{G1} - \frac{1}{\lambda}I_A^{G1} + N_A^{G1} + (\delta_A^G + \delta^{G1}) + \varepsilon_A^{G1} \tag{1}$$

where G1 is an index of the GPS satellite, A is an index of a receiver, Φ_A^{G1} is a phase observation, λ is a wave length, ρ_A^{G1} is a geometrical distance between satellite and the receiver in meters, dt_A is a receiver clock error, dt^{G1} is a satellite clock error, T_A^{G1} is a tropospheric delay in meters, I_A^{G1} - is a ionospheric delay in meters, N_A^{G1} is a ambiguity, δ_A^G is a receiver hardware delay, δ^{G1} is a satellite hardware delay and ε_A^{G1} is a measurement noise. In (1), in the receiver hardware delay, we can find an upper index G. It was used to show that this particular delay applies only to the GPS system. If we add a second receiver, B, and a second satellite, G2, we can create a DD. This allows us to eliminate the receiver and satellite clock errors and hardware delays (Leick et al., 2015):

$$\Phi_{AB}^{G1G2} = \frac{1}{\lambda}\rho_{AB}^{G1G2} + \frac{1}{\lambda}T_{AB}^{G1G2} - \frac{1}{\lambda}I_{AB}^{G1G2} + N_{AB}^{G1G2} + \varepsilon_{AB}^{G1G2} \tag{2}$$

For the same receivers A and B, the phase observations equation and DD observations equations for Galileo satellites E1 and E2 can be presented as follows:

$$\Phi_A^{E1} = \frac{1}{\lambda}\rho_A^{E1} + (dt_A - dt^{E1}) + \frac{1}{\lambda}T_A^{E1} - \frac{1}{\lambda}I_A^{E1} + N_A^{E1} + (\delta_A^E + \delta^{E1}) + \varepsilon_A^{E1} \tag{3}$$

$$\Phi_{AB}^{E1E2} = \frac{1}{\lambda}\rho_{AB}^{E1E2} + \frac{1}{\lambda}T_{AB}^{E1E2} - \frac{1}{\lambda}I_{AB}^{E1E2} + N_{AB}^{E1E2} + \varepsilon_{AB}^{E1E2} \tag{4}$$

δ_A^E in (3) is a hardware delay that applies only to a Galileo. It was eliminated while creating DD observations with two Galileo satellites. This is because each system's correlation process occurs separately in the receiver, which causes different delays. The double-differenced observations equation for receiver A and B and GPS satellite G1 (used as a reference satellite) and Galileo satellite E1 can be written as follows:

$$\Phi_{AB}^{G1E1} = \frac{1}{\lambda}\rho_{AB}^{G1E1} + \frac{1}{\lambda}T_{AB}^{G1E1} - \frac{1}{\lambda}I_{AB}^{G1E1} + N_{AB}^{G1E1} + \delta_{AB}^{GE} + \varepsilon_{AB}^{G1E1} \tag{5}$$

The term δ_{AB}^{GE} in (5) can be associated with ISB. Since hardware delay is not eliminated, it must be considered during the positioning process. Odijk & Teunissen (2013) have already detailed the process of eliminating ISB using classical methods (with ambiguity resolution). In this article, a different method of incorporating ISB into the mathematical model will be presented. The ionospheric and tropospheric delays can be easily modelled and introduced as known parameters. Also, for short baselines, like those used during the test in this paper, the influence of atmospheric delays is meagre and can be omitted.

Inter-System Bias in MAFA method

The MAFA (Modified Ambiguity Function Approach) employs a least-square estimation approach with conditional equations within the functional model for processing GNSS carrier phase observations. Conditional equations allow for the elimination of ambiguity in a mathematical model. However, the integer character of the ambiguities is preserved. The equation (5) can be rewritten as follows (Teunissen & Kleusberg, 1998):

$$\Phi_{AB}^{G1E1} = \frac{1}{\lambda}\rho(\mathbf{x}_r)_{AB}^{G1E1} + ISB_c + N_{AB}^{G1E1} + e_{AB}^{G1E1} \tag{6}$$

where G1 is a reference satellite for both GPS and Galileo systems, E1 is a Galileo satellite, $\mathbf{x}_r$ is a coordinates vector of the receiver and Inter-System Bias, e_{AB}^{G1E1} is the observation error (measurement noise), ISB_c is an Inter-System Bias identical with δ_{AB}^{GE} in (5). The influence of the ionosphere and troposphere was omitted because the receivers used in the experiment are very close to each other. This proximity renders the impact of these two parameters negligible. In the case of more considerable distances between receivers, the effects of the ionosphere and troposphere can be estimated and incorporated into the mathematical model. The nominal accuracy of phase observation measurements is usually set at about 0.01 cycles. This means that corrections should be significantly less than 0.5 cycles of the measured phase. Considering the integer nature of the ambiguities and assuming that observation errors are less than half a cycle, we can rewrite equation (6) as follows (Cellmer et al., 2018):

$$e_{AB}^{G1E1} = \left(\Phi_{AB}^{G1E1} - \frac{1}{\lambda}\rho(\mathbf{x}_r)_{AB}^{G1E1} - ISB_c\right) - \mathrm{int}\left(\Phi_{AB}^{G1E1} - \frac{1}{\lambda}\rho(\mathbf{x}_r)_{AB}^{G1E1} - ISB_c\right) \tag{7}$$

where "int" denotes rounding to the nearest integer value. The linearized form of equation (7) can be written as follows (Cellmer et al., 2018):

$$\mathbf{e}_{ISB} = \boldsymbol{\delta}_{ISB} - \frac{1}{\lambda}\mathbf{A}_{\mathbf{MISB}}\mathbf{dx}_{\mathbf{r}} \tag{8}$$

Where $\mathbf{e}_{ISB}$ is the residual vector, $\mathbf{dx}_{\mathbf{r}}$ is a parameter vector, $\boldsymbol{\delta}_{ISB}$ is the misclosures vector, $\mathbf{A}_{\mathbf{MISB}}$ is the design matrix. The design matrix must consist of four columns. The

first three columns are derivatives derived from the Taylor series expansion, and the fourth column is dedicated to ISB estimation:

$$\mathbf{A_{MISB}} = \begin{bmatrix} a_x^{G1G2} & a_y^{G1G2} & a_z^{G1G2} & 0 \\ a_x^{G1G3} & a_y^{G1G3} & a_z^{G1G3} & 0 \\ \vdots & \vdots & \vdots & \vdots \\ a_x^{G1G_m} & a_y^{G1G_m} & a_z^{G1G_m} & 0 \\ a_x^{G1E1} & a_y^{G1E1} & a_z^{G1E1} & 1 \\ a_x^{G1E2} & a_y^{G1E2} & a_z^{G1E2} & 1 \\ \vdots & \vdots & \vdots & \vdots \\ a_x^{G1E_m} & a_y^{G1E_m} & a_z^{G1E_m} & 1 \end{bmatrix} \tag{9}$$

where G_m is the number of GPS satellites and E_m is the number of observed Galileo satellites. The fourth column consists of: 0 for GPS to GPS DD and 1 for Galileo to GPS DD. In the classical model, to estimate the ISB parameter, it is necessary to link the ISB with ambiguity, which is not the case here. To form the free terms vector, the following equation is used (Kwaśniak et al., 2017):

$$\boldsymbol{\delta}_{\mathbf{ISB}} = \left(\boldsymbol{\Phi} - \frac{1}{\lambda}\boldsymbol{\rho}(\mathbf{x}_r^0) - \mathbf{ISB_{c0}} \right) - \mathrm{int}\left(\boldsymbol{\Phi} - \frac{1}{\lambda}\boldsymbol{\rho}(\mathbf{x}_r^0) - \mathbf{ISB_{c0}} \right) \tag{10}$$

where: $\boldsymbol{\Phi}$ is the DD phase observations vector, $\boldsymbol{\rho}(\mathbf{x}_r^0)$ is the vector of DD geometrical distances based on approximate position, $\mathbf{ISB_{c0}}$ is a vector of approximate values of the ISB. The solution is sought using the least-squares method to minimize the following objective function:

$$\Psi = \mathbf{e}_{ISB}^T \mathbf{P} \mathbf{e}_{ISB} \tag{11}$$

where **P** is a weight matrix. To estimate the parameter vector, the following formula must be used:

$$\mathbf{d\breve{x}}_r = \lambda \left(\mathbf{A_{MISB}}^T \mathbf{P} \mathbf{A_M} \right)^{-1} \mathbf{A_{MISB}}^T \mathbf{P} \boldsymbol{\delta}_{\mathbf{ISB}} \tag{12}$$

and to estimate the residual vector we use the following formula:

$$\breve{\mathbf{e}}_{ISB} = \boldsymbol{\delta}_{\mathbf{ISB}} - \frac{1}{\lambda}\mathbf{A_{MISB}} \mathbf{d\breve{x}}_r \tag{13}$$

The key to the proper functioning of the MAFA method is the implementation of a search procedure. In equation (7), the term N_{AB}^{G1E1} is replaced by $\mathrm{int}\left(\Phi_{AB}^{G1E1} - \frac{1}{\lambda}\rho(\mathbf{x}_r)_{AB}^{G1E1} \right)$. But it can only be done by fulfilling the two conditions. The first condition says the approximate position must be within the correct pull-in region (Cellmer et al., 2018; 2021). The pull-in region can be defined using a Voronoi cell (Xu, 2006). According to the second condition, the residuals should be less than 0.5 cycles. The search process is

conducted within the domain of four variables: the three coordinates (x, y, z) and ISB. The search region is created as an error hyperellipsoid of the approximated position and approximated ISB, using covariance matrix $\mathbf{Q}_{\mathbf{x}}$ of these parameters. Inside that hyperellipsoid, the grid of the candidates is formed. The orientation of the grid is compatible with the main axes of the error hyperellipsoid. The density of the grid must be set appropriately. The search procedure will require extensive computation if the grid is too dense. If it is too sparse, the Voronoi cell of the correct position and value of ISB might be missed. This issue has been extensively investigated by Cellmer et al. (2021). The size of the error hyperellipsoid is determined by the chosen confidence level. The hyperellipsoid is described by several parameters: its centre, the lengths of its main axes, and the orientations of these axes (Cellmer et al., 2017). The centre of the error hyperellipsoid is located at the a priori position and a priori ISB. The lengths of the main axes can be computed using the following equations:

$$r_x = \sqrt{\frac{\chi_r^2}{\mu_x}}, r_y = \sqrt{\frac{\chi_r^2}{\mu_y}}, r_z = \sqrt{\frac{\chi_r^2}{\mu_z}}, r_{ISB} = \sqrt{\frac{\chi_r^2}{\mu_{ISB}}} \tag{14}$$

where χ_r^2 is a critical value of χ^2 distribution with 4 degrees of freedom, $\mu_x, \mu_y, \mu_z, \mu_{ISB}$ are eigenvalues of the matrix $\mathbf{Q}_{\mathbf{x}}^{-1}$. The lengths of the error hyperellipsoid axes are determined by the relationship between the assumed confidence level p_0 and the critical value χ_c^2 of the χ^2 distribution with 4 degrees of freedom (Cellmer et al., 2018). Each candidate is tested. They each serve as an approximate position, and the criterion given by equation (11) is then checked. The candidate that minimizes this criterion is selected, and the estimation result based on this candidate is the final solution in the MAFA method. The results of the estimation is a position and the value of Inter-System Bias. The correctness of determining the ISB values by the MAFA method was verified by comparing the obtained results with the LAMBDA method and by comparing them with the results obtained by Tian et al. (2020) who also tested a few of the pairs used in an experiment. A comparison was made with a LAMBDA method and with results obtained by Tian et al. to verify whether the obtained results were correct and could be used for further analyses.

Experiment design

During the tests, 20 permanent IGS (International GNSS Service) stations were used (Table 1). These stations were organized into ten pairs, and calculations were carried out for each pair. Among these pairs, three consisted of the same type of receivers, while the remaining seven pairs comprised receivers of different types. For pairs of the same type of receivers, the ISB should be zero. This is because the hardware delays on both receivers should be identical. In the case of two different types of receivers, these delays vary, which means that the ISB can but does not necessarily reach values up to half a cycle. The selection of pairs ensured that the distance between the receivers did not

exceed 5 km, thereby minimizing the impact of atmospheric conditions on the results. In the first part of the tests, the calculations were carried out for 5-epoch sessions, using 24-hour observations data from February 9, 2021. The elevation mask was 15°. During the computational process, the position was determined, and the ISB was estimated. The L1 and E1, as well as L5 and E5a observations, were used. The test aimed to examine the stability of ISB over one day. During the second part of the tests, data from October 16, 2020, January 2, 2021, February 10 and 11, 2021, March 21, 2021, and June 19, 2021, were used. For the data from the first two and the last two days, the ISB value was determined in a single six-hour static session. For data from February 10 and 11, the ISB was determined four times for six-hour static sessions, i.e., 0:00-6:00, 6:00-12:00, 12:00-18:00, and 18:00-24:00 UTC. This was done to check the stability of the ISB value for consecutive adjacent days. The remaining obtained results are intended to allow an assessment of the long-term stability of the ISB. There was a lack of data on some days because the pairs consisted of different receivers (even if only one of the receivers is changed, different ISB values will be obtained). For WTZR-WTZ2, LCK3-LCK4, and NCKU-CKSV pairs, the reference ISB value is 0.000 m. Also, for TLSE-TLSG and SUTH-SUTM, where the pair consists of different receivers, the reference ISB value is 0.000 m. For JOZE-JOZ2 pair it is -0.001 m. For PTAG-PTGG, STJO-STJ3, and NTUS-SIN1, the reference ISB value is 0.094 m. For ROAG-SFER, it is -0.095 m. These values were determined in long 12 hours static sessions and adopted as reference values.

Table 1. Pairs of receivers used in test

Reference station	Rover	Reference station receiver	Rover receiver	Distance [m]
WTZR	WTZ2	LEICA GR50 4.31/7.403	LEICA GR50 4.31/7.403	69
LCK3	LCK4	TRIMBLE ALLOY 5.43	TRIMBLE ALLOY 5.43	4
NCKU	CKSV	TRIMBLE NETR9 5.37	TRIMBLE ALLOY Nav 5.44/Boot5.44	361
JOZE	JOZ2	SEPT POLARX5 5.3.2	TRIMBLE NETR9 5.45	84
TLSE	TLSG	TRIMBLE NETR9 5.45	SEPT POLARX5TR 5.4.0	1266
SUTH	SUTM	SEPT POLARX5 5.4.0	JAVAD TRE_3 3.7.10	142
ROAG	SFER	SEPT POLARX5TR 5.3.	LEICA GR25 4.31/6.713	124
PTAG	PTGG	LEICA GR50 4.31/7.403	SEPT POLARX5 5.4.0	54
STJO	STJ3	JAVAD TRE_3N DELTA 3.7.5p1	SEPT POLARX5TR 5.4.0	47
NTUS	SIN1	LEICA GR50 4.20/7.300	TRIMBLE NETR9 5.45	317

Source: authors work

Results and discussion

In Figure 1, the results of ISB estimation for pairs of identical receivers are presented. The obtained ISB values are expressed in meters. For this purpose, the obtained results in cycles were multiplied by the wavelength. Here, we can observe that the determined values of the ISB oscillate around the value of 0.000 m, and except for

a few outliers, they lie within the range of ±1 cm. Results obtained by Paziewski et al. (2015) show similar accuracy, about ±2 cm for L1. Odijk & Teunissen (2013) also achieve an accuracy ±2 cm for both L1/E1 and L5/E5a frequencies. Table 2 shows the mean values and STD (standard deviations). It can be observed that the standard deviations for all three pairs do not exceed 1 cm. The variability in the estimated ISB values results from errors in the estimation outcomes based on small samples (i.e., five epoch sessions). The obtained means are identical to the assumed reference values for both frequencies. We can observe bigger outliers for L5/E5a frequency than for L1/E1. This was due to the still limited number of available satellites with L5 observations. Sometimes, only three satellites were available, further weakening the estimation process.

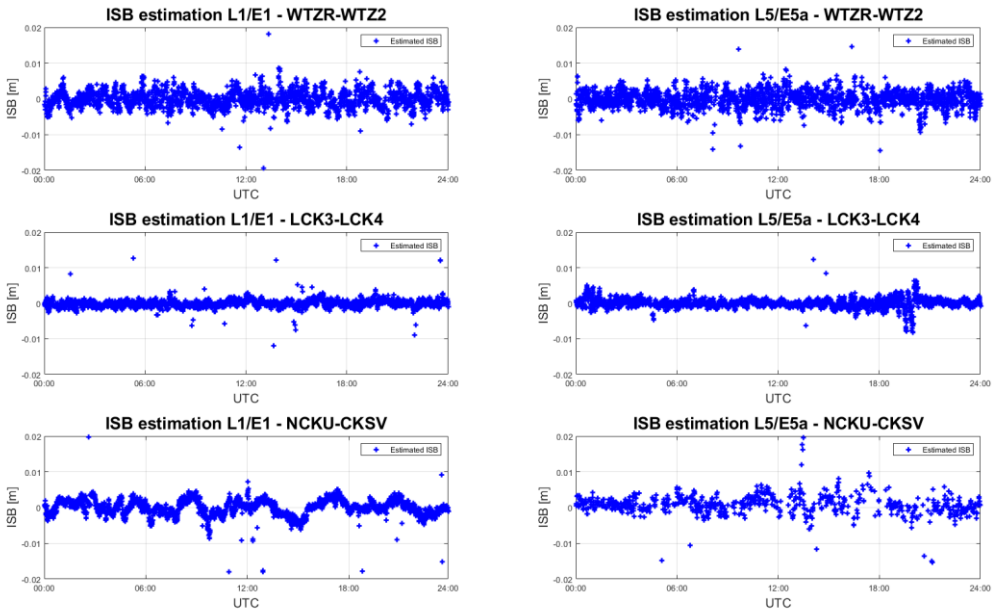

Fig. 1. ISB estimation for same type receiver pairs:
WTZR-WTZ2, LCK3-LCK4, NCKU-CKSV
Source: own work

Figure 2 presents the results of the ISB estimation for pairs of different receivers where the ISB values are zero or close to zero. Similar to the previous case, we can observe that the estimated ISB values oscillate around zero for both frequencies. Table 2 also shows that the mean values of the results are close to zero. It also can be observed that the standard deviations for all three pairs again do not exceed 1 cm. Also, in this case, the obtained means are identical to the assumed reference values for both frequencies.

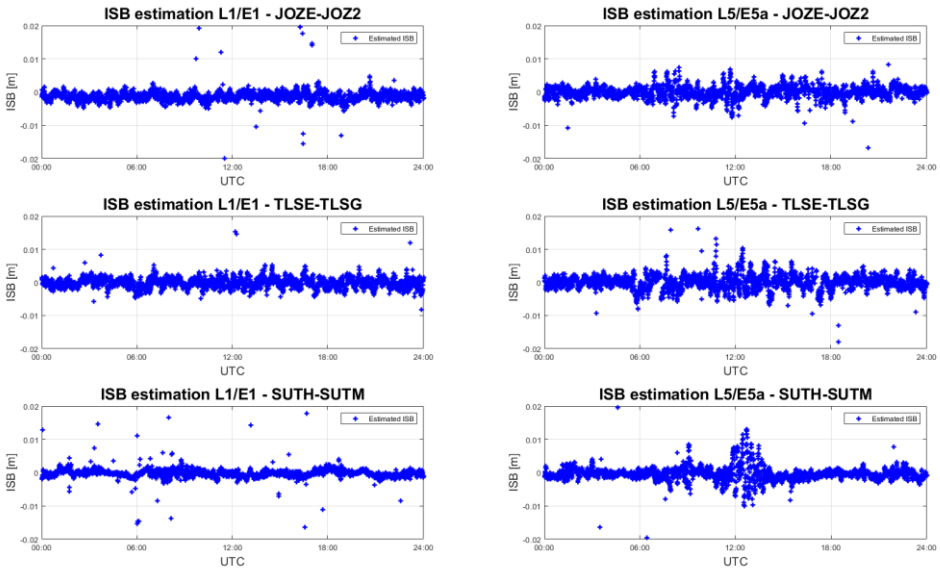

Fig. 2. ISB estimation for different type receiver pairs:
JOZE-JOZ2, TLSE-TLSG, SUTH-SUTM
Source: authors work

Table 2. Mean and standard deviation for post-processing RTK
Inter-System Bias estimation

Pair	L1/E1		L5/E5a	
	mean [m]	STD [m]	mean [m]	STD [m]
WTZR-WTZ2	0.000	0.007	0.000	0.010
LCK3-LCK4	0.000	0.006	0.000	0.005
NCKU-CKSV	0.000	0.007	0.001	0.007
JOZE-JOZ2	-0.001	0.002	0.000	0.004
TLSE-TLSG	0.000	0.003	0.000	0.004
SUTH-SUTM	0.000	0.003	0.000	0.003
ROAG-SFER	-0.095	0.001	0.000	0.002
PTAG-PTGG	0.094	0.003	0.000	0.004
STJO-STJ3	0.094	0.003	0.000	0.004
NTUS-SIN1	0.094	0.002	0.001	0.004

Source: authors work

Figure 3 presents the results for pairs of receivers where the ISB assumes significant values – around half the cycle. Table 2 shows that the standard deviation values do not exceed 5 mm, and the mean values obtained are identical or slightly different from reference values. The results indicated that the ISB value remains constant for short time intervals and no drifts can be observed. This applies to both the L1/E1 and L5/E5a frequencies. Analyzing the obtained results from the ISB estimation, we can observe no

trend in the estimated values for 24 hours. Therefore, it can be assumed that the estimated ISB values are constant for 24 hours. Similarly, the results presented in Figures 2 and 3 show that the more prominent outliers observed for the L5/E5a frequency are due to the sometimes low number of available GPS satellites with L5 observations.

As observed in Tables 3 and 4, for all pairs of receivers, the estimated ISB values for February 10 and 11, 2021, for the L1/E1 frequency are identical or differ by a maximum of 2 millimeters compared to those obtained on February 9. For the L5/E5a frequency, all the obtained results are identical to the reference values from February 9. Unfortunately, data for each experimental day was only available for three pairs of receivers: LCK3-LCK4, JOZE-JOZ2, and ROAG-SFER. Analyzing the results from Tables 3 and 4 for these three pairs, as well as the results obtained for the other stations, it can be observed that the ISB values for the L1/E1 frequency for the analyzed days are similar or identical to those obtained on February 9, 2021. In the case of the L5/E5a frequency, almost all pairs yielded identical results to the reference values. The results obtained correspond to results by Odijk & Teunissen (2013) and Li et al. (2021) which indicates that ISB is stable both in the short term and in the long term. Analyzing the obtained results, it can be assumed that the ISB parameter value is constant for a specific pair of GNSS receivers over time. The outliers observed in Figures 1, 2 and 3 arise as a result of low accuracy obtained during the estimation. It is because 5-second sessions were used, and estimating the ISB parameter and posit burdens the mathematical model. However, the goal was to demonstrate the overall stability of this parameter and the lack of any drift in the obtained results. Even after several months, its value does not change. This allows for the assumption that once the ISB value is determined, it can be used in calculations as a constant parameter for a specific pair of receivers.

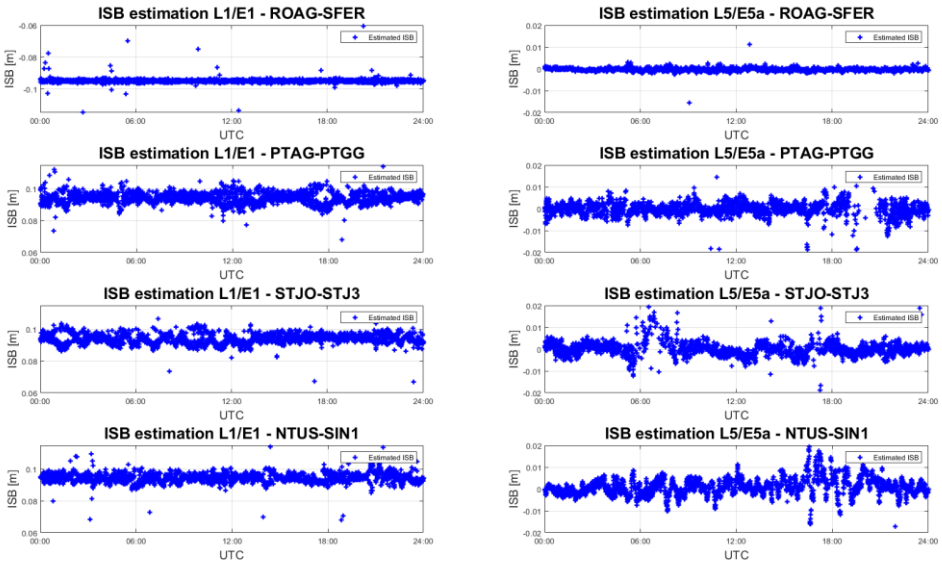

Fig. 3. ISB estimation for different type receiver pairs:
ROAG-SFER, PTAG-PTGG, STJO-STJ3, NTUS-SIN1
Source: authors work

Table 3. The estimation results for ISB for October 16, 2020, January 2, 2021, February 10 and 11, 2021, March 21, 2021, and June 19, 2021, in relation to the results from February 9, 2021, for the L1/E1 frequency

L1/E1										
	WTZR - WTZ2	LCK3 - LCK4	NCKU - CKSV	JOZE - JOZ2	TLSE - TLSG	SUTH - SUTM	ROAG - SFER	PTAG - PTGG	STJO - STJ3	NTUS - SIN1
2020 10 16	0.000	0.000	no data	-0.001	no data	no data	0.095	no data	no data	0.094
2021 01 02	0.000	0.000	0.000	-0.002	no data	no data	0.095	no data	no data	0.095
2021 02 09	0.000	0.000	0.000	-0.002	0.000	0.000	-0.095	0.097	0.095	0.095
2021 02 10	0.000	0.000	0.000	-0.002	0.000	0.000	-0.095	0.097	0.095	0.095
	0.000	0.000	0.000	-0.002	0.000	0.000	-0.096	-0.095	0.095	0.096
	0.000	0.000	0.000	-0.001	0.000	0.000	0.095	0.095	0.094	0.096
	0.000	0.000	-0.001	-0.001	0.000	0.000	0.095	-0.095	0.094	0.096
2021 02 11	0.000	0.000	0.000	-0.002	0.000	0.000	-0.095	0.096	0.095	0.096
	0.000	0.000	0.000	-0.001	0.000	0.000	0.095	-0.095	0.094	0.096
	0.000	0.000	0.000	-0.001	0.000	0.000	0.095	-0.095	0.094	-0.096
	0.000	0.000	0.000	-0.001	0.000	0.000	0.095	0.095	-0.096	0.095
2021 03 21	0.000	no data	no data	-0.001	0.000	0.000	0.095	0.095	0.096	0.095
2021 06 19	no data	0.000	no data	-0.001	0.000	0.000	0.095	0.096	no data	no data

Source: authors work

Table 4. The estimation results for ISB for October 16, 2020, January 2, 2021, February 10 and 11, 2021, March 21, 2021, and June 19, 2021, in relation to the results from February 9, 2021, for the L5/E5a frequency

L5/E5a										
	WTZR - WTZ2	LCK3 - LCK4	NCKU - CKSV	JOZE - JOZ2	TLSE - TLSG	SUTH - SUTM	ROAG - SFER	PTAG - PTGG	STJO - STJ3	NTUS - SIN1
2020 10 16	0.000	0.000	no data	0.000	no data	no data	0.000	no data	no data	0.001
2021 01 02	0.000	0.000	0.000	0.000	no data	no data	0.000	no data	no data	0.000
2021 02 09	0.000	0.000	0.000	0.000	0.000	0.000	0.000	0.000	0.000	0.000
2021 02 10	0.000	0.000	0.000	0.000	0.000	0.000	0.000	0.000	0.000	0.000
	0.000	0.000	0.000	0.000	0.000	0.000	0.000	0.000	0.000	0.000
	0.000	0.000	0.000	0.000	0.000	0.000	0.000	0.000	0.000	0.000
	0.000	0.000	0.000	0.000	0.000	0.000	0.000	0.000	0.000	0.000
2021 02 11	0.000	0.000	0.000	0.000	0.000	0.000	0.000	0.000	0.000	0.000
	0.000	0.000	0.000	0.000	0.000	0.000	0.000	0.000	0.000	0.000
	0.000	0.000	0.000	0.000	0.000	0.000	0.000	0.000	0.000	0.000
	0.000	0.000	0.000	0.000	0.000	0.000	0.000	0.000	0.000	0.000
2021 03 21	0.000	no data	no data	0.001	0.000	0.000	0.000	0.000	0.000	0.000
2021 06 19	no data	0.000	no data	0.000	0.000	0.000	0.000	0.000	no data	no data

Source: authors work

Conclusions and summary

In this paper, the stability of the Inter-System Bias was tested. The modified MAFA method was used to estimate the ISB values. Tests were performed on 20 IGS stations. The ten pairs of receivers were created. Three of those pairs consisted of the same type receivers. The remaining seven pairs consisted of different types of receivers. The ISB was estimated for a GPS-Galileo combination with L1/E1 and L5/E5a combinations. In the first part of the test, the daily stability of ISB was tested. The results showed that for a single day, the ISB remains stable and does not change its value. This applies to both L1/E1 and L5/E5a frequencies. In the second part of the test, the long-term stability was tested. The obtained results show that Inter-System Bias is stable not only in a few days but also over several months. This also applies to both L1/E1 and L5/E5a frequencies. The tests also showed that the MAFA method can be successfully used to determine the value of ISB.

Acknowledgements

This research was supported by the grant “An algorithm of common processing of observations from various GNSS systems including the estimation of inter-system Bias“ 2017/27/N/ST10/00412 with agreement number: UMO-2017/27/N/ST10/00412 from Narodowe Centrum Nauki (National Science Center), Poland.

References

Cellmer S., Nowel K., Kwaśniak D. (2017). Optimization of a Grid of Candidates in the Search Procedure of the MAFA Method. Environmental Engineering. Proceedings of the International Conference on Environmental Engineering. ICEE, vol. 10, pp. 1–7, 10.3846/enviro.2017.179.

Cellmer S., Nowel K., Kwaśniak D. (2018). The New Search Method in Precise GNSS Positioning. IEEE Transactions on Aerospace and Electronic Systems, 54(1), 404–415, DOI: 10.1109/TAES.2017.2760578.

Cellmer S., Nowel K., Fischer A. (2021). A search step optimization in an ambiguity function-based GNSS precise positioning. Survey Review, 1–8, DOI: 10.1080/00396265.2021.1885947.

Håkansson M., Jensen A., Horemuž M., Hedling G. (2017). Review of code and phase biases in multi-GNSS positioning. GPS Solutions. 21. 10.1007/s10291-016-0572-7.

Kwaśniak D., Cellmer S., Nowel K., (2017). Precise positioning in Europe using the Galileo and GPS combination. 10.3846/enviro.2017.210.

Kwaśniak D., Cellmer S. (2021). Incorporating Inter-System Bias in Single Point Positioning Based on GPS, Galileo and BeiDou System. Geomatics and Environmental Engineering. 15. 97. 10.7494/geom.2021.15.1.97.

Leick A., Rapoport L., Tatarnikov D. (2015). GPS Satellite Surveying. John Wiley & Sons, DOI: 10.1002/9781119018612.

Li W., Zhu S., Ming Z. (2021). Estimation of Inter-System Biases between BDS-3/GPS/Galileo and Its Application in RTK Positioning. Remote Sensing, 13(17), 3507, DOI: 10.3390/rs13173507.

Li M., Rovira G., Nie W., Xu T., Xu G. (2023). Inter-system biases solution strategies in multi-GNSS kinematic precise point positioning. GPS Solutions. 27. 10.1007/s10291-023-01443-3.

Liu X., Jiang W., Li Pa, Deng Z., Ge M., Schuh H. (2022). An extended inter-system biases model for multi-GNSS precise point positioning. Measurement. 206. 112306. 10.1016/j.measurement.2022.112306.

Odijk D., Teunissen P. (2013) Characterization of Between-Receiver GPS-Galileo Inter-System Biases and their Effect on Mixed Ambiguity Resolution. GPS Solutions, 17(4), 521-533, DOI: 10.1007/s10291-012-0298-0.

Paziewski J., Wielgosz P. (2015). Accounting for Galileo-GPS inter-system biases in precise satellite positioning. Journal of Geodesy, 89(1), 81-93, DOI: 10.1007/s00190 014 0763-3.

Paziewski J., Wielgosz P. (2017). Investigation of some selected strategies for multi-GNSS instantaneous RTK positioning. Advances in Space Research, 59(1), 12 23, DOI: 10.1016/j.asr.2016.08.034.

Paziewski J., Sieradzki R., Wielgosz P. (2015). Selected properties of GPS and Galileo-IOV receiver intersystem biases in multi-GNSS data processing. Measurement Science and Technology. 26. 095008. 10.1088/0957-0233/26/9/095008.

Tian Y., Sui L., Xiao G., Zhao D., Chai H., Liu C. (2020). Estimating inter-system biases for tightly combined Galileo/BDS/GPS RTK, Advances in Space Research, vol. 65, no. 1, pp. 572–585, https://doi.org/10.1016/j.asr.2019.09.003.

Teunissen P., Kleusberg A. (1998) GPS for Geodesy. Springer – Verlag, Berlin Heidelberg New York.

Xu P. (2006). Voronoi cells, probabilistic bounds, and hypothesis testing in mixed integer linear models. IEEE Transactions on Information Theory 52(7):3122–3138.

Xu C,. Wang H., Dang Y., Chen H., Zhang L. (2015). Unified Estimation Model of Multi-system Biases Including BDS/GPS/GLONASS/Galileo. In: J. Sun, J. Liu, S. Fan, X. Lu, (ed.), China Satellite Navigation Conference (CSNC) 2015 Proceedings: Volume I. Lecture Notes in Electrical Engineering, vol 340. Springer, Berlin, Heidelberg. https://doi.org/10.1007/978-3-662-46638-4_23.

Zang N., Li B., Nie L., Shen Y. (2019). Inter-system and inter-frequency code biases:simultaneous estimation, daily stability and applications in multi-GNSS single-frequency precise point positioning. GPS Solutions. 24. 10.1007/s10291-019-0926-z.

Zeng A., Yang Y., Ming F. (2017). BDS–GPS inter-system bias of code observation and its preliminary analysis. GPS Solut 21, 1573–1581, https://doi.org/10.1007/s10291-017-0636-3.

Zhu S., Li W. (2021). Performances Analysis of Tightly-Combined Multi-system RTK Positioning with BDS-3/GPS/Galileo. 10.1007/978-981-16-3138-2_56.